

HONG YONG SOHN and DE-QIU FAN

It is argued in this paper that the initial rate should not be used for the measurement or analysis the kinetics of a fluid–solid reaction, especially for a reaction in which the effect of pore diffusion starts appearing even moderately as the reaction proceeds. Even in the absence of external mass transfer effects, it is shown in this work by rigorous mathematical analysis that the range of conditions where the initial rate represents the intrinsic kinetics is very narrow. For an initially non-porous solid in the absence of external mass transfer effects, the very initial rate should mathematically be the intrinsic rate even when pore diffusion becomes important as the reaction proceeds. However, even in this case, the range of conditions for this statement is very limited. For the reaction of an initially porous solid, the rate at time zero is already affected by pore diffusion unless its effect is negligible over the entire range of conversion. Furthermore, the initial reaction rates of porous solids reacting under large values of k/D_e ratio (chemical reactivity is much greater than the capacity for pore diffusion) have an apparent rate constant of $\sqrt{k \cdot D_e}$ and thus pore diffusion alone does not control the initial rate no matter how large the effect of pore diffusion is overall.

DOI: 10.1007/s11663-017-0940-x

© The Minerals, Metals & Materials Society and ASM International 2017

I. INTRODUCTION

FLUID–SOLID reactions play a major role in many important chemical and metallurgical processes. A large amount of work has been devoted to the kinetics of fluid–solid reactions. The reader is referred to the literature^[1] for a comprehensive discussion of this topic. The investigation of reaction kinetics often relies on the initial rates.^[2–6] [Also see the numerous sources and sites found by googling with the term ‘initial rate method.’] The initial rate method is appropriate for the determination of kinetics of homogeneous reactions, often saving time and effort. But as will be shown in this paper, the initial rate should not be used for the measurement or analysis of the kinetics of a fluid–solid reaction, especially for a reaction in which the effect of pore diffusion starts appearing even moderately as the reaction proceeds. The following analysis of the initial rate of a gas–solid reaction is based on an isothermal system. The heat transfer effect, which makes the analysis even less reliable, is not taken into consideration in this analysis.

Typically, the rate of a fluid–solid reaction is measured under a fixed concentration of the fluid reactant with mass transfer effects eliminated under a sufficiently high fluid velocity. Let us consider the following general fluid–solid reaction:



II. AN INITIALLY NON-POROUS SOLID FORMING A POROUS PRODUCT LAYER (THE SHRINKING-CORE SYSTEM)

A schematic representation of this reaction system is shown in Figure 1.

In this case, the exact conversion vs time relationship is given in the following dimensionless form for the three basis geometries (large slabs, long cylinders, and spheres)^[1,8]:

$$t^* = g_{F_p}(X) + \sigma_s^2 [p_{F_p}(X) + 4X/Sh^*], \quad [2]$$

where

$$g_{F_p}(X) = 1 - (1 - X)^{1/F_p}$$

$$p_{F_p}(X) = 1 - \frac{F_p(1 - X)^{2/F_p} - 2(1 - X)}{F_p - 2}$$

The specific form of $p_{F_p}(X)$ for the three basic geometries is:

$$p_{F_p}(X) = \begin{cases} X^2 & F_p = 1 \\ X + (1 - X) \ln(1 - X) & F_p = 2 \\ 1 - 3(1 - X)^{2/3} + 2(1 - X) & F_p = 3 \end{cases}$$

with

$$t^* = \frac{bk}{\rho_s} \frac{A_p}{F_p V_p} \left(C_{A0} - \frac{C_{C0}}{K} \right) t$$

$$\sigma_s^2 = \frac{k}{2D_e} \frac{V_p}{A_p} \left(1 + \frac{1}{K} \right)$$

HONG YONG SOHN and DE-QIU FAN are with the Department of Metallurgical Engineering, University of Utah, Salt Lake City, UT, 84112. Contact e-mail: h.y.sohn@utah.edu

Manuscript submitted December 6, 2016.

Article published online February 15, 2017.

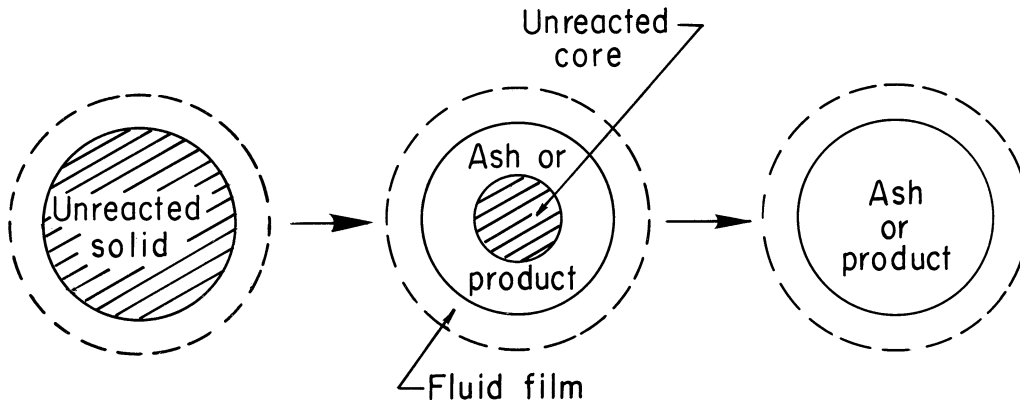


Fig. 1—Schematic representation of the reaction of an initially non-porous solid forming a porous product layer (the shrinking-core system). Reprinted from Ref. [9].

$$Sh^* = \frac{h_D}{D_e} (2F_p V_p / A_p)$$

here, σ_s^2 is the shrinking-core reaction modulus, which represents a ratio of chemical reactivity and capacity for pore diffusion. A large σ_s^2 signifies that the overall rate is diffusion-controlled, while a small σ_s^2 represent the cases of chemical reaction control.

In Eq. [2], the $g_{F_p}(X)$ arises from the contribution of chemical reaction and is the conversion function under chemical reaction control; the $p_{F_p}(X)$ arises from the contribution of pore diffusion in the product layer and is the conversion function under pore diffusion control.

The rate of conversion in terms of the extent of reaction can be readily derived from Eq. [2], as follows:

$$\frac{dX}{dt^*} = \left[g'_{F_p}(X) + \sigma_s^2 \left(p'_{F_p}(X) + \frac{4}{Sh^*} \right) \right]^{-1} \quad [3]$$

The initial rate is when $X = 0$, at which point $g'_{F_p}(X) = 1/F_p$ and $p'_{F_p}(X) = 0$, thus signifying the absence of pore diffusion effect and the fact that the initial rate in the shrinking-core system is controlled by chemical reaction and external mass transfer. The initial rate is thus given by:

$$\left. \frac{dX}{dt} \right|_{t=0} = \frac{bk(C_{A0} - \frac{C_{C0}}{K})}{\rho_s \left(1 + \frac{k}{h_D} \left(1 + \frac{1}{K} \right) \right)} \frac{A_p}{V_p} \quad [4]$$

In the absence of external mass transfer effect ($Sh^* \rightarrow \infty$), Eq. [4] is simplified to:

$$\left. \frac{dX}{dt} \right|_{t=0} = \frac{bk(C_{A0} - C_{C0}/K)}{\rho_s} \left(\frac{A_p}{V_p} \right) \quad [5]$$

Equation [5] can be further rearranged to obtain the molar rate of solid consumption per area of the sample as:

$$R_r = - \left. \frac{\rho_s V_p}{A_p} \frac{d(1-X)}{dt} \right|_{t=0} = b \cdot k (C_{A0} - C_{C0}/K) \quad [6]$$

As expected, this equation indicates that the initial rate per unit area is independent of the shape or size of the solid.

It is shown from Eq. [6] that the rate constant obtained from the initial rate is the intrinsic value. It is noted that a first-order chemical reaction is assumed in the above derivation for convenience, but the same result applies to non-first-order fluid–solid reaction is:

$$R_r = - \left. \frac{\rho_s V_p}{A_p} \frac{d(1-X)}{dt} \right|_{t=0} = b \cdot k \cdot f(C_A^n, C_C^{cn}) \quad [7]$$

In practice, the determination of the initial rate requires measurements until the solid achieves a certain degree of reaction, *i.e.*, up to a certain value of X . This value of X will depend on the value of σ_s^2 . To evaluate this, the rate in Eq. [3] in the absence of external mass transfer effect is plotted as a function of fraction conversion X in Figure 2. It is seen that for σ_s^2 less than 0.1, the reaction rate is not significantly affected by pore diffusion until conversion reaches 5 to 10 pct, and up to this range of conversion, the rate can still be approximated as initial rate. However, it would be very difficult to obtain the intrinsic kinetics from the initial rate when there is even a relatively moderate effect of pore diffusion ($\sigma_s^2 > 0.1$) in the overall rate, even though the mathematical equation, Eq. [6], indicates that the rate at $X = 0$ is the intrinsic rate in this system in the absence of external mass transfer effect. Further, with external mass transfer effect in place, it would be even more difficult to obtain the intrinsic rate constant, as shown in Eq. [4], especially for reactions with small equilibrium constants K .

III. AN INITIALLY POROUS SOLID FORMING A POROUS PRODUCT LAYER

For the reaction of a porous solid, the grain model^[1,7] that assumes idealized solid structure made up of individual grains will be used for the derivation of the initial reaction rate. The choice of this model is just for the purpose of illustration and the general conclusion drawn by the analysis performed in this work is valid

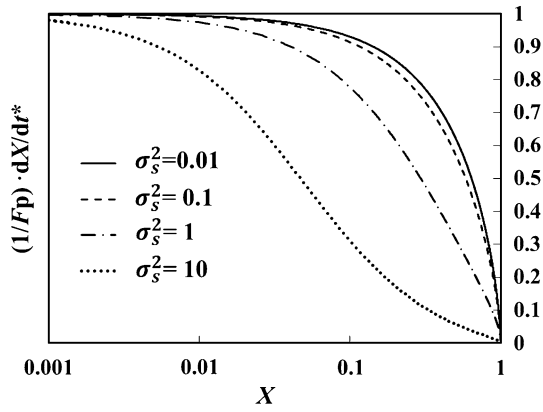


Fig. 2— $(1/F_p)dX/dt^*$ vs X for different values of σ_s^2 with $F_p = 3$ for an initially non-porous solids with $Sh^* \rightarrow \infty$.

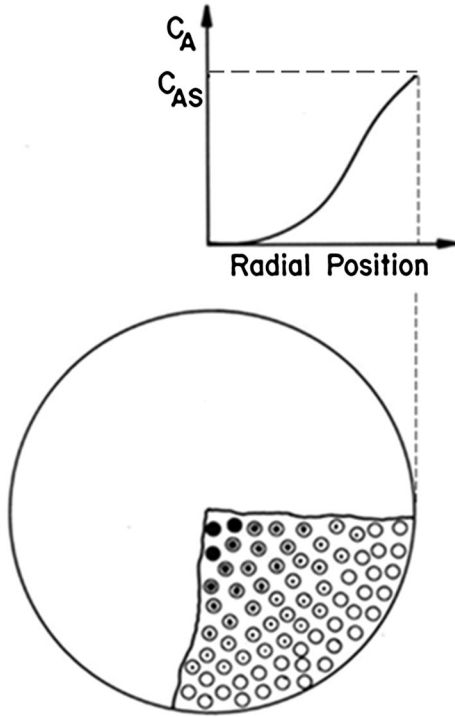


Fig. 3—Schematic representation of a porous solid with unreacted grains. Reprinted from Ref. [9].

regardless of the model used to describe the reaction of an initially porous solid with a fluid. In the grain model, the grains react according to chemically controlled shrinking-core system. Although this idealization is not necessary and can be relaxed, grain model facilitates the analysis and will not affect the conclusions made here. A schematic representation of a porous solid with unreacted grains is shown in Figure 3.

The equation that governs the fluid diffusion and chemical reaction of a porous solid is given as follows, assuming pseudo-steady state and equal effective diffusivity of gaseous species A and C:

$$D_e \nabla^2 C_A - v_A = 0 \quad [8]$$

$$D_e \nabla^2 C_C + v_A = 0 \quad [9]$$

By dividing Eq. [9] by K and subtracting from Eq. [8]:

$$D_e \nabla^2 (C_A - C_C/K) - v_A(1 + 1/K) = 0 \quad [10]$$

Although not necessary for this discussion, it is convenient to rewrite Eq. [10] in dimensionless form by introducing the following normalized variables:

$$\begin{aligned} \psi &= (C_A - C_C/K) / (C_{A0} - C_{C0}/K) \\ t^* &= \frac{bk}{\rho_s} \left(\frac{A_g}{F_g V_g} \right) \left(C_{A0} - \frac{C_{C0}}{K} \right) t \\ \hat{\sigma}^2 &= \frac{1}{2F_p} \left(\frac{F_p V_p}{A_p} \right)^2 \left(\frac{A_g}{F_g V_g} \right) \frac{(1-\epsilon)k}{D_e} \left(1 + \frac{1}{K} \right) \\ \xi &= \frac{A_g r_c}{F_g V_g} \\ \eta &= \frac{A_p R}{F_p V_p} \end{aligned} \quad [11]$$

The above particular definition of $\hat{\sigma}$, which represents a ratio of the capacities for pore diffusion and chemical reaction, has been shown to be very convenient in that it makes the numerical criteria for chemical or pore diffusion control identical for all nine combinations of F_g and F_p .^[1,8]

Equation [10] now becomes

$$\frac{1}{\eta^{F_p-1}} \frac{d}{d\eta} \left(\eta^{F_p-1} \frac{d\psi}{d\eta} \right) - 2F_g F_p \cdot \hat{\sigma}^2 \psi \cdot \xi^{F_g-1} = 0 \quad [12]$$

At $t = 0$, all the grains are unreacted as shown in Figure 3 and ξ is unity everywhere throughout the particle. Thus, Eq. [12] becomes:

$$\frac{1}{\eta^{F_p-1}} \frac{d}{d\eta} \left(\eta^{F_p-1} \frac{d\psi}{d\eta} \right) - 2F_g F_p \cdot \hat{\sigma}^2 \psi = 0 \quad \text{at } t = X = 0 \quad [13]$$

This equation can be solved for different values of F_p by rearranging it into a Bessel's equation:

$$\eta^2 \frac{d^2 \psi}{d\eta^2} + (F_p - 1) \eta \frac{d\psi}{d\eta} - 2F_g F_p \hat{\sigma}^2 \cdot \eta^2 \psi = 0 \quad \text{at } t = X = 0 \quad [14]$$

with the following boundary conditions:

$$\begin{cases} \frac{d\psi}{d\eta} = Sh^*(1 - \psi)/2 & \text{at } \eta = 1 \\ \frac{d\psi}{d\eta} = 0 & \text{at } \eta = 0 \end{cases}$$

Equation [14] can be solved analytically to yield the following general solution:

$$\psi = \eta^{\frac{2-F_p}{2}} \left[c_1 \cdot I_{\frac{|2-F_p|}{2}}(\sqrt{2F_p F_g} \hat{\sigma} \cdot \eta) + c_2 \cdot I_{-\frac{|2-F_p|}{2}}(\sqrt{2F_p F_g} \hat{\sigma} \cdot \eta) \right], \quad [15]$$

where c_1 and c_2 are constants to be determined based on the boundary conditions. The solutions for particles of different shape factors are listed in Table I.

Table I. Analytical Solutions at $t = 0$ with External Mass Transfer Effects

F_p	Analytical Solution at $t = 0$	dX/dt^* at $t = 0$
1	$\psi = \frac{Sh^* \cosh(\sqrt{2F_p F_g} \hat{\sigma} \eta)}{Sh^* \cosh(\sqrt{2F_p F_g} \hat{\sigma}) + 2\sqrt{2F_p F_g} \hat{\sigma} \sinh(\sqrt{2F_p F_g} \hat{\sigma})}$	$\frac{dX}{dt^*} = \frac{Sh^* \cdot \sqrt{2F_p F_g} \tanh(\sqrt{2F_p F_g} \hat{\sigma})}{2Sh^* \cdot \hat{\sigma} + 4\sqrt{2F_p F_g} \tanh(\sqrt{2F_p F_g} \hat{\sigma})}$
2	$\psi = \frac{Sh^* \cdot I_0(\sqrt{2F_p F_g} \hat{\sigma} \eta)}{2\sqrt{m} \hat{\sigma} I_1(\sqrt{2F_p F_g} \hat{\sigma}) + Sh^* \cdot I_0(\sqrt{2F_p F_g} \hat{\sigma})}$	$\frac{dX}{dt^*} = \frac{1}{2\hat{\sigma}} \frac{Sh^* \sqrt{2F_p F_g} I_1(\sqrt{2F_p F_g} \hat{\sigma})}{2\sqrt{2F_p F_g} \hat{\sigma} \cdot I_1(\sqrt{2F_p F_g} \hat{\sigma}) + Sh^* \cdot I_0(\sqrt{2F_p F_g} \hat{\sigma})}$
3	$\psi = \frac{Sh^* \cdot \sinh(\sqrt{2F_p F_g} \hat{\sigma} \eta)}{2\sqrt{2F_p F_g} \hat{\sigma} \cosh(\sqrt{2F_p F_g} \hat{\sigma}) \eta + (Sh^* - 2) \sinh(\sqrt{2F_p F_g} \hat{\sigma}) \eta}$	$\frac{dX}{dt^*} = \frac{Sh^*}{2\hat{\sigma}^2} \frac{\sqrt{2F_p F_g} \hat{\sigma} \coth(\sqrt{2F_p F_g} \hat{\sigma}) - 1}{2\sqrt{2F_p F_g} \hat{\sigma} \coth(\sqrt{2F_p F_g} \hat{\sigma}) + Sh^* - 2}$

Table II. Analytical Solutions at $t = 0$ in the Absence of External Mass Transfer Effects

F_p	Analytical Solution at $t = 0$	dX/dt^* $t = 0$
1	$\psi = \frac{\cosh(\sqrt{2F_p F_g} \hat{\sigma} \eta)}{\cosh(\sqrt{2F_p F_g} \hat{\sigma})}$	$\frac{dX}{dt^*} = \frac{\sqrt{2F_p F_g} \sinh(\sqrt{2F_p F_g} \hat{\sigma})}{2\hat{\sigma} \cosh(\sqrt{2F_p F_g} \hat{\sigma})}$
2	$\psi = \frac{I_0(\sqrt{2F_p F_g} \hat{\sigma} \eta)}{I_0(\sqrt{2F_p F_g} \hat{\sigma})}$	$\frac{dX}{dt^*} = \frac{\sqrt{2F_p F_g} I_1(\sqrt{2F_p F_g} \hat{\sigma})}{2\hat{\sigma} I_0(\sqrt{2F_p F_g} \hat{\sigma})}$
3	$\psi = \frac{\sinh(\sqrt{2F_p F_g} \hat{\sigma} \eta)}{\eta \sinh(\sqrt{2F_p F_g} \hat{\sigma})}$	$\frac{dX}{dt^*} = \frac{1}{2\hat{\sigma}^2} \left[\frac{\cosh(\sqrt{2F_p F_g} \hat{\sigma})}{\sinh(\sqrt{2F_p F_g} \hat{\sigma})} \sqrt{2F_p F_g} \hat{\sigma} - 1 \right]$

In the absence of external mass transfer effect ($Sh^* \rightarrow \infty$), the above analytical solutions are simplified as follows:

Unlike the initial rate of a non-porous solid following the shrinking-core model, the analytical solutions for $X = t = 0$ in Tables I and II show general dependence on pore diffusion. Under the pseudo-steady state approximation, the overall reaction rate is equal to the rate of diffusion of fluid reactant into the particle:

$$\frac{(1 - \varepsilon)\rho_s V_p}{b} \frac{dX}{dt} = D_e A_p \left. \frac{dC_A}{dR} \right|_{R=F_p V_p / A_p} \quad [16]$$

The dimensionless form of which is:

$$\frac{dX}{dt^*} = \frac{1}{2\hat{\sigma}^2} \left. \frac{d\psi}{d\eta} \right|_{\eta=1} \quad [17]$$

The derivations of the above equations are given in the literature^[1] and the reader is referred to it for details. The initial rates in Table I under the two asymptotic cases of no pore diffusion effect ($\hat{\sigma} \rightarrow 0$) and pore diffusion control ($\hat{\sigma} \rightarrow \infty$) become:

$$\lim_{\hat{\sigma} \rightarrow 0} \left. \frac{dX}{dt^*} \right|_{t=0} = F_g \quad [18]$$

$$\lim_{\hat{\sigma} \rightarrow \infty} \left. \frac{dX}{dt^*} \right|_{t=0} = \frac{1}{2\hat{\sigma}} \frac{Sh^* \sqrt{2F_p F_g}}{Sh^* + 2\sqrt{2F_p F_g} \hat{\sigma}} \quad [19]$$

It is seen from Eq. [18] that the initial rates for particles of different shapes are independent of external mass transfer effect when pore diffusion effect is negligible. The initial rates dX/dt^* in Table II ($Sh^* \rightarrow \infty$) for particles of different shapes are plotted as a function of

$\hat{\sigma}^2$ in Figure 4 with $\hat{\sigma} < 1$. It is shown that the initial rates of particles of different overall shapes become the same as $\hat{\sigma}^2$ approaches 0 as indicated by Eq. [18]. The initial rates for particles of different shapes when there is a significant effect of pore diffusion and the effect of external mass transfer is negligible are presented in Figure 5. In this case, the initial rates described by Eq. [19] converge to the following asymptote:

$$\lim_{\hat{\sigma} \rightarrow \infty} \left. \frac{dX}{dt^*} \right|_{t=0} = \frac{\sqrt{2F_p F_g}}{2\hat{\sigma}} \quad [20]$$

Further, the expressions of the asymptotic rates in terms of molar rate of solid consumption per area of the external surface in the absence of the effect of external mass transfer are given by

$$\begin{aligned} R_r &= - \left. \frac{\rho_s V_p (1 - \varepsilon)}{A_p} \frac{d(1 - X)}{dt} \right|_{t=0} \\ &= bk(C_{As} - C_{Cs}/K) \frac{(1 - \varepsilon)A_g}{V_g} \\ &= b \cdot k \cdot f(C_A, C_C) \cdot S_v \end{aligned} \quad [21]$$

$$\begin{aligned} R_r &= - \left. \frac{\rho_s V_p (1 - \varepsilon)}{A_p} \frac{d(1 - X)}{dt} \right|_{t=0} \\ &= \sqrt{k \cdot D_e} \cdot \frac{b}{\sqrt{1 + 1/K}} \left(\frac{(1 - \varepsilon)A_g}{V_g} \right)^{\frac{1}{2}} \left(C_{As} - \frac{C_{Cs}}{K} \right) \\ &= b \frac{\sqrt{k \cdot D_e} \cdot S_v}{\sqrt{1 + 1/K}} \cdot f(C_A, C_C) = \frac{b \cdot k_{app}}{\sqrt{1 + 1/K}} \cdot f(C_A, C_C), \end{aligned} \quad [22]$$

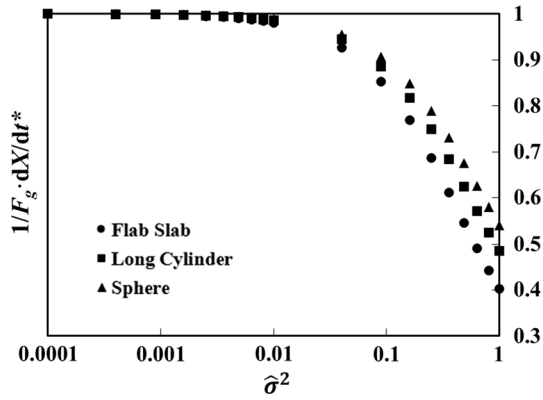


Fig. 4—Initial reaction rates for particles of different shapes with $\hat{\sigma}^2 < 1$ and $F_g = 3$.

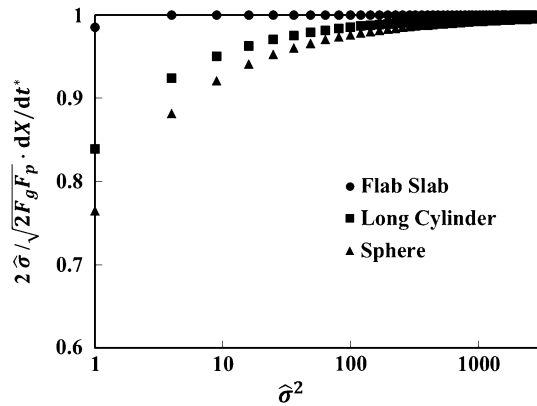


Fig. 5—Initial reaction rates for particles of different shape with $\hat{\sigma}^2 > 1$ and $F_g = 3$.

where S_v is the surface area per unit volume of porous solid, a quantity readily measured, *e.g.*, by the BET method. These equations indicate that the initial rate per unit area of external surface is independent of the shape or size of the pellet.

It is noted that the initial reaction rate of porous solids will represent the intrinsic reaction rate only when $\hat{\sigma} \rightarrow 0$, as shown by Eq. [21]. However, the initial rate for a porous solid with some effects of pore diffusion ($\hat{\sigma}^2 > 0.1$) will be significantly affected by pore diffusion, and thus does not represent the intrinsic reaction rate, as shown in Figures 3 and 4 as well as by Eq. [22]. Moreover, the effect external mass transfer would make it even more difficult to obtain the intrinsic rate constant when the effect of pore diffusion is in place. It is of interest to note that even in the case of $\hat{\sigma} \rightarrow \infty$ and $Sh^* \rightarrow \infty$, the initial rate of a porous solid is not controlled by pore diffusion alone; rather it is controlled equally by pore diffusivity and chemical reactivity represented by the $\sqrt{k \cdot D_e}$ term.

The relationship between the apparent activation energy when $\hat{\sigma} \rightarrow \infty$ and the true activation energy for an irreversible reaction (large K) or when K is a weak function of temperature can be derived by taking the

natural logarithm of Eq. [22] (neglecting the usually weak temperature dependence of D_e):

$$\ln(R_r) = \ln(\sqrt{k}) + \text{const} = \ln(k_{\text{app}}) + \text{const} \quad [23]$$

Substituting the reaction rate constants in Eq. [23] with their Arrhenius expressions:

$$\begin{aligned} & -\frac{1}{2} \frac{E_T}{RT} + \frac{1}{2} \ln(A_T) + \text{const} \\ & = -\frac{E_{\text{app}}}{RT} + \ln(A_{\text{app}}) + \text{const} \end{aligned} \quad [24]$$

It is seen from Eq. [24] that the value of the apparent activation energy when $\hat{\sigma} \rightarrow \infty$ is related to the true activation energy by:

$$E_{\text{app}} = \frac{1}{2} E_T \quad [25]$$

The ratio of the apparent activation energy for an intermediate value of $\hat{\sigma}^2$ and the true activation energy should lie between one half and unity (for large or weakly temperature dependent K). This result is also observed in reactions in catalyst pellets^[10] and also in the reactions of porous solids that produce no solid product layer.^[11] Although not shown here, the apparent reaction order with respect to the fluid reactant concentration is also falsified for a non-first-order reaction.^[10,11]

IV. CONCLUDING REMARKS

To summarize, the following points should be kept in mind when considering initial rates of an isothermal fluid–solid reactions:

1. Mathematically, the initial rate (at $X = 0$) of reaction of an initially non-porous solid represents the intrinsic reaction rate, regardless of the value of σ_s^2 . Up to what extent of solid conversion this condition applies depends on the value of σ_s^2 for the system, as shown in Figure 2. The results shown in this figure indicates that it would be very difficult to obtain the intrinsic kinetics from the initial rate when there is even a relatively moderate effect of pore diffusion ($\sigma_s^2 > 0.1$) in the overall rate, even though the mathematical equation indicates that the rate at $X = 0$ is the intrinsic rate in this system (in the absence of external mass transfer effect).
2. The initial rate of a porous solid is in general affected by pore diffusion. When $\hat{\sigma}^2 < 0.01$, however, the initial rate (in fact the rate over the entire conversion) will equal the intrinsic rate. Even for $\hat{\sigma}^2$ as small as 0.1, the initial rate of an initially porous solid is significantly affected by pore diffusion, and thus not controlled by intrinsic chemical reaction. When $\hat{\sigma}^2 > 10$, the apparent rate constant for the initial rate will be $\sqrt{k \cdot D_e}$. Additionally, pore diffusion alone does not control the initial rate no matter how large the ratio of k/D_e becomes. (In this case, reactions that produce porous product layer will eventually be rate-controlled by pore diffusion as the product layer builds up.)

3. Besides fluid–solid reactions often encounter, an induction period in the initial stage of reaction, during which the reaction mechanism applicable to the main reaction is not applicable. The existence of this induction period would make it much more difficult to determine the intrinsic reaction rate constant for the main reaction based on the initial rate. Another factor that sometimes makes the measurement of the initial rate difficult is the time taken for the concentration of gas to be uniform through the reactor once the gas is switched to the reactant gas in isothermal experiments. Moreover, the transient period for the reactive gas to reach the pseudo-steady state profile inside the pores of the solid particle at the beginning of an experiment may affect the accuracy of determining the initial rates. These other factors are usually negligible for reactions with moderate rates, but can be significant for fast reactions.

NOMENCLATURE

A_g	Surface area of the grain (m^2)
A_p	External surface area of the particle (m^2)
A_{app}	Apparent pre-exponential factor
A_T	Real pre-exponential factor
b	Stoichiometric coefficient of solid reactant
D_e	Effective diffusivity in the porous product layer ($m^2 s^{-1}$)
E_{app}	Apparent activation energy ($kJ \cdot mol^{-1}$)
E_T	Real activation energy ($kJ \cdot mol^{-1}$)
F_g	Grain shape factor, which takes 1 for flat slabs, 2 for long cylinders and 3 for spheres
F_p	Particle shape factor for the solid particle, which takes 1 for flat slabs, 2 for long cylinders and 3 for spheres
I	Modified Bessel function of the first kind
k	Intrinsic reaction rate constant ($m s^{-1}$)
k_{app}	Apparent reaction rate constant ($m s^{-1}$)

K	equilibrium constant for the reaction
R_r	initial molar rate of consumption per unit area of solid surface ($mol s^{-1} m^{-2}$)
Sh^*	The modified Sherwood number
S_v	Surface area per unit volume of porous solid (m^{-1})
t^*	The dimensionless time
V_p	Volume of the particle (m^3)
V_g	Volume of the grain (m^3)
X	Fractional conversion of the solid reactant
ε	Porosity of the particle
η	Dimensionless particle radius
ξ	Dimensionless grain radius
ρ_s	Molar density of the solid reactant ($mol m^{-3}$)
σ_s^2	Shrinking-core reaction modulus
ψ	Dimensionless gaseous concentration

REFERENCES

1. J. Szekely, J.W. Evans, and H.Y. Sohn: *Gas–Solid Reactions*, Academic Press, New York, 1976.
2. M.R. Usman, D.L. Cresswell, and A.A. Garforth: *ISRN Chem. Eng.*, 2013, Article ID 152893, <http://dx.doi.org/10.1155/2013/152893>.
3. L. Wu, S. Tong, and M. Ge: *J. Phys. Chem. A*, 2013, vol. 117, pp. 4937–44.
4. G.P. Mathur and G. Thodos: *Chem. Eng. Sci.*, 1966, vol. 21, pp. 1191–1200.
5. J. Casado, M.A. Lopez-Quintela, and F.M. Lorenzo-Barral: *J. Chem. Educ.*, 1986, vol. 63, pp. 450–52.
6. A.C. Lasaga: *Kinetic Theory in the Earth Sciences*, Princeton University Press, Princeton, NJ, 1998, pp. 31–37.
7. H.Y. Sohn, J. Szekely: *Chem. Eng. Sci.*, 1972, vol. 72, pp. 763–78.
8. H.Y. Sohn: *Reaction Engineering Models, Treatise on Process Metallurgy, Volume 3 Industrial Processes Part A*, Elsevier, Oxford, 2014, vol. 3, pp. 758–810.
9. H.Y. Sohn: *MetallTrans. B*, 1991, vol. 22, pp. 737–54.
10. E.E. Petersen: *Chemical Reaction Analysis*, Prentice-Hall, Englewood Cliffs, NJ, 1965.
11. J. Szekely, J.W. Evans, and H.Y. Sohn: *Gas–Solid Reactions*, Academic Press, New York, 1976, pp. 116–17.